

## Electronic Supplementary Information

# Elevated Amyloidoses of Human IAPP and Amyloid Beta by Lipopolysaccharide and Their Mitigation by Carbon Quantum Dots

Kairi Koppel,<sup>a</sup> Huayuan Tang,<sup>b</sup> Ibrahim Javed,<sup>c</sup> Mehrdad Parsa,<sup>d</sup> Monika Mortimer,<sup>e</sup> Thomas P. Davis,<sup>a,c\*</sup> Sijie Lin,<sup>f</sup> Alan L. Chaffee,<sup>d</sup> Feng Ding<sup>b\*</sup> and Pu Chun Ke<sup>g,a\*</sup>

<sup>a</sup> ARC Centre of Excellence in Convergent Bio-Nano Science and Technology, Monash Institute of Pharmaceutical Sciences, Monash University, 381 Royal Parade, Parkville, VIC 3052, Australia

<sup>b</sup> Department of Physics and Astronomy, Clemson University, Clemson, SC 29634, USA

<sup>c</sup> Australian Institute for Bioengineering and Nanotechnology, The University of Queensland, Brisbane Qld 4072, Australia

<sup>d</sup> School of Chemistry, Monash University, 17 Rainforest Walk, Clayton, VIC 3800, Australia

<sup>e</sup> Institute of Environmental and Health Sciences, College of Quality and Safety Engineering, China Jiliang University, Hangzhou, Zhejiang 310018, China

<sup>f</sup> College of Environmental Science and Engineering, State Key Laboratory of Pollution Control and Resource Reuse, Tongji University, 1239 Siping Road, Shanghai 200092, China

<sup>g</sup> Zhongshan Hospital, Fudan University, 111 Yixueyuan Rd, Xuhui District, Shanghai, 200032, China

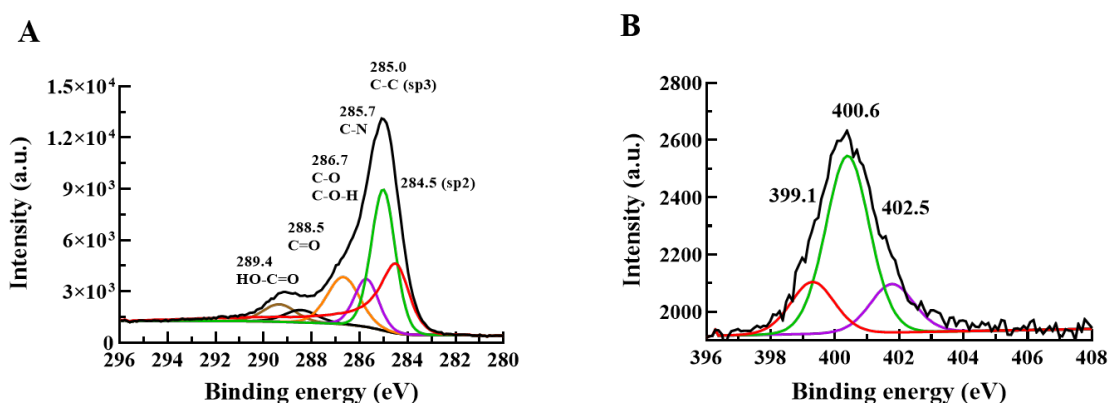


**Figure S1. High-resolution XPS spectra of CQDs. (A) C 1 s and (B) N 1 s.**

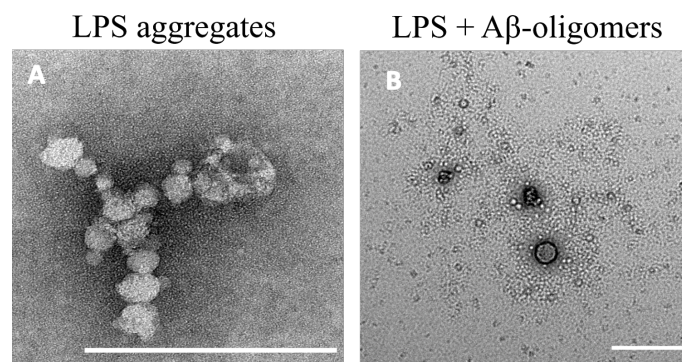


**Figure S2.** TEM imaging of LPS and A $\beta$  interacting with LPS of different conformations. LPS aggregates (A), LPS micelles surrounded by A $\beta$  monomers (B). Scale bars: 200 nm.

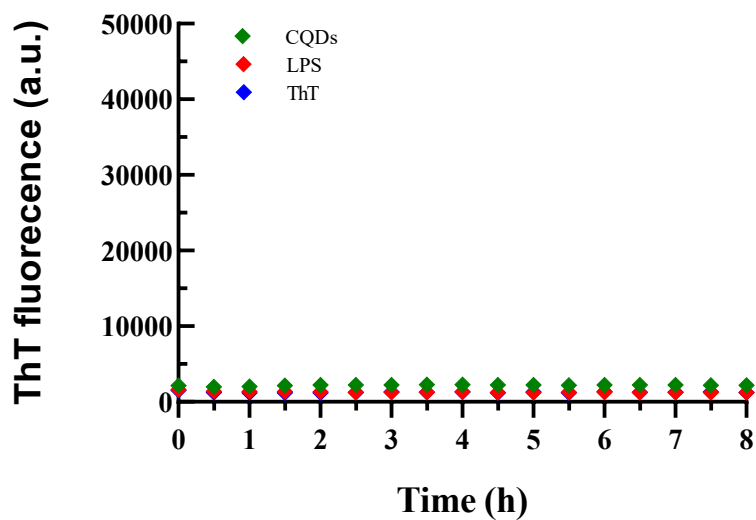


**Figure S3.** ThT fluorescence of CQDs, LPS and ThT dye. CQDs, LPS and ThT concentrations are as follows: 200  $\mu$ g/mL, 0.78  $\mu$ g/mL and 100  $\mu$ M. Excitation/emission: 440/484 nm.

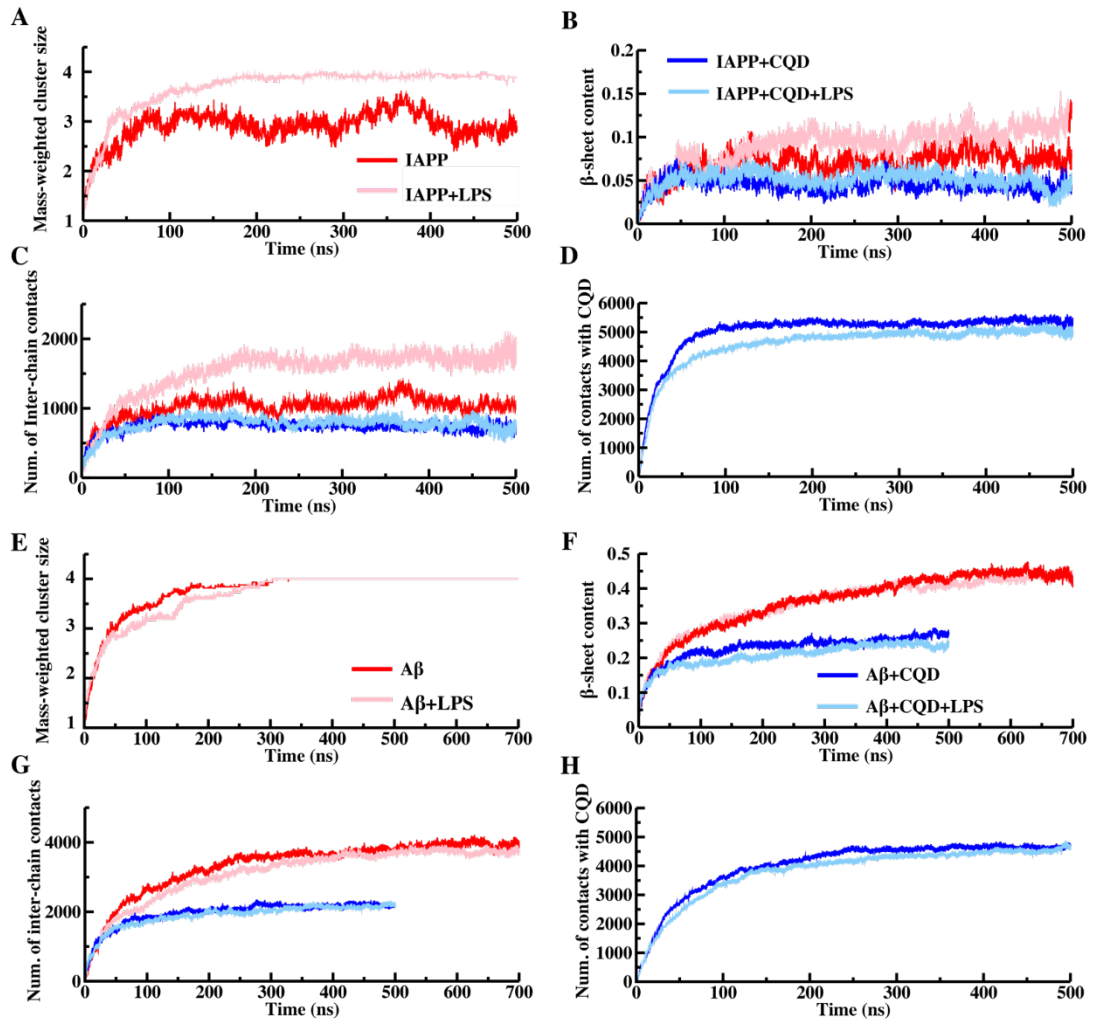


**Figure S4. Dynamics of the aggregation processes of IAPP (A-D) and Aβ (E-H).** The mass-weighted cluster size (A), β-sheet content (B), number of inter-chain contacts (C) and number of contacts between peptides and a CQD (D) for the systems with IAPP. The mass-weighted cluster size (E), β-sheet content (F), number of inter-chain contacts (G) and number of contacts between peptides and the CQD (H) for the systems with Aβ.

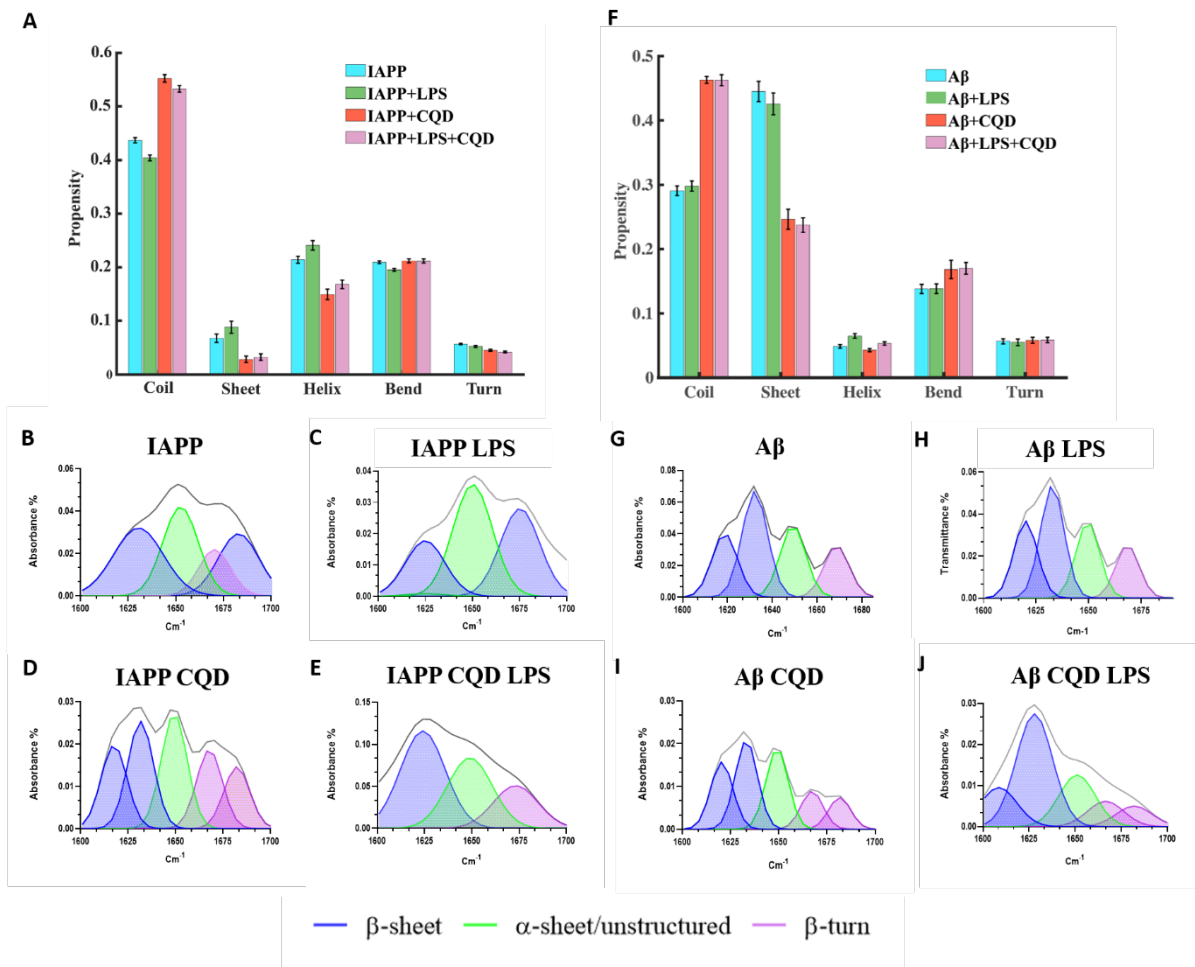


**Figure S5. Analysis of the secondary structures of IAPP and Aβ in the presence of LPS and CQDs. DMD simulations (top row) and FTIR spectral deconvolution analysis (bottom row).**

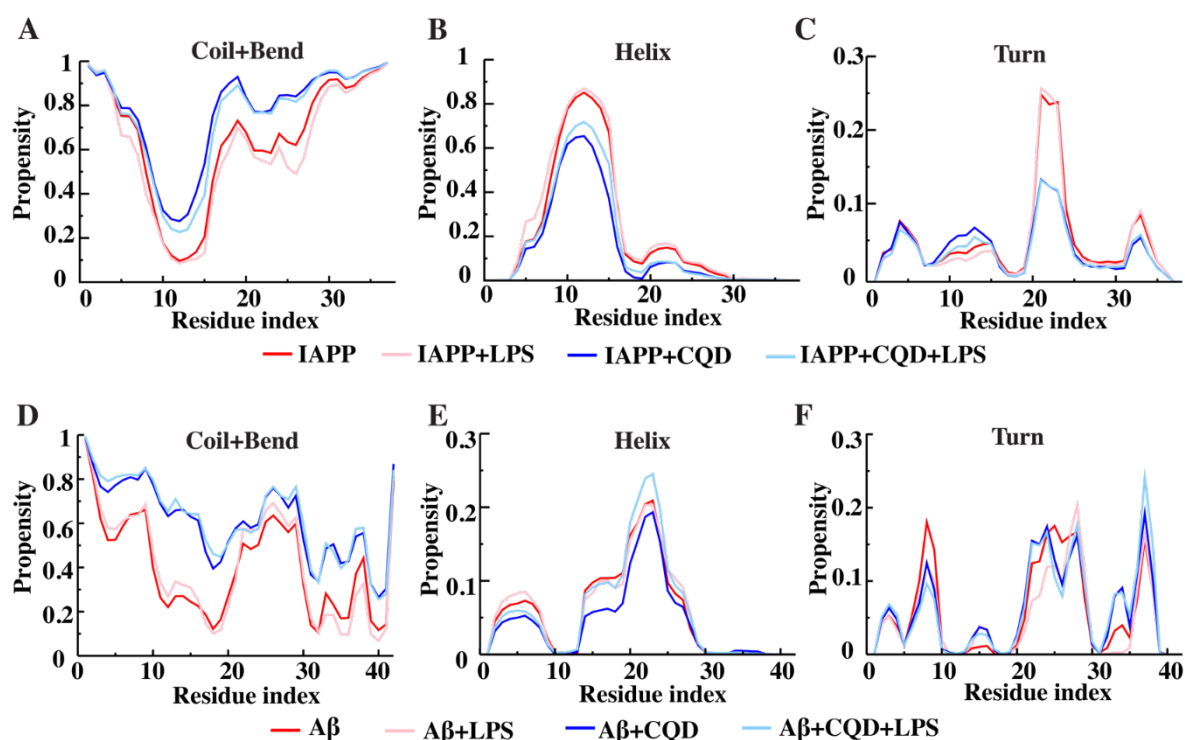


**Figure S6. *In silico* IAPP and A $\beta$  secondary structure analyses.** The rises in the  $\beta$ -sheet contents in the peptides in the presence of LPS at residues 16-20 and 24-32 were due to the reduction in the propensity of unstructured coils and bends (A-C, Fig. 3C). For A $\beta$ , its  $\beta$ -sheet content was specifically promoted in the regions with strong LPS binding (residues 16-21 and 31-40), and reduced in other regions (D-F, Fig. 3D). The reduction was likely a result of additional electrostatic interactions between the negatively charged A $\beta$  and LPS. For both IAPP (A-C) and A $\beta$  (D-F), CQDs reduced their  $\beta$ -sheet propensities by increasing the coil and bend structures.

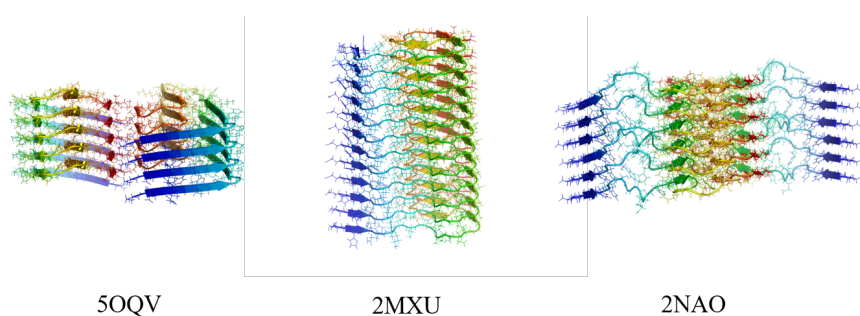


**Figure S7. Examples of solved A $\beta$  fibril structures.** For each of the PDB structures, the individual peptide is shown in cartoon and colored in rainbow, highlighting the formation of in-registered parallel  $\beta$ -sheet between adjacent peptides in the fibril.

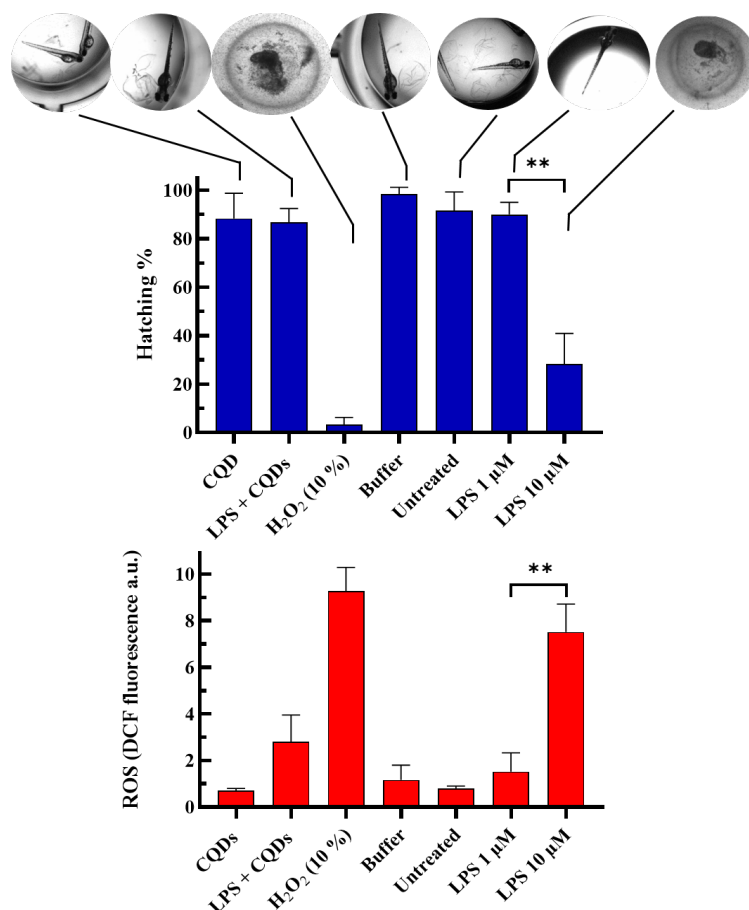


**Figure S8. Hatching rates and ROS levels of zebrafish exposed to control treatments.** LPS (10 and 1 μM), CQDs (0.5 μg/mL), and LPS (1 μM) with CQDs (0.5 μg/mL), IAPP (10 μM) or Aβ (10 μM) were microinjected to the embryos. The embryos were imaged at 3 h post injection under the green and bright field channels of a fluorescence microscope. ROS production was measured 12 h after injections. Hatching of the embryos was calculated at 3 days post injection. P<0.005 \*\*

**Table S1. Band assignments in FTIR spectroscopy<sup>1</sup>**

Secondary structure	Band wavenumber (cm <sup>-1</sup> )
α-helix	1648 - 1657
β-sheet	1623 - 1641, 1674 - 1695, 1615 - 1627
β-turns	1622 - 1686
Unstructured	1642 - 1657

## References

1. B. Srour, S. Bruechert, S. L. A. Andrade and P. Hellwig, *Methods Mol. Biol.*, 2017, **1635**, 195-203.